Journal of Power Sources 196 (2011) 9618–9624

Contents lists available at ScienceDirect

Journal of Power Sources

journal homepage: www.elsevier.com/locate/jpowsour

A fast synthesis of $Li_3V_2(PO_4)_3$ crystals via glass-ceramic processing and their battery performance

Kenta Nagamine, Tsuyoshi Honma, Takayuki Komatsu*

Department of Materials Science and Technology, Nagaoka University of Technology, 1603-1 Kamitomioka-cho, Nagaoka 940-2188, Japan

ARTICLE INFO

Article history:
Received 23 May 2011
Received in revised form 24 June 2011
Accepted 27 June 2011
Available online 2 July 2011

Keywords:
Lithium ion secondary battery
Lithium vanadium phosphate
Glass-ceramic

ABSTRACT

A synthesis of $Li_3V_2(PO_4)_3$ being a potential cathode material for lithium ion batteries was attempted via a glass-ceramic processing. A glass with the composition of $37.5Li_2O$–$25V_2O_5$–$37.5P_2O_5$ (mol%) was prepared by a melt-quenching method and precursor glass powders were crystallized with/without 10 wt% glucose in N_2 or 7%H_2/Ar atmosphere. It was found that heat treatments with glucose at 700 °C in 7%H_2/Ar can produce well-crystallized $Li_3V_2(PO_4)_3$ in the short time of 30 min. The battery performance measurements revealed that the precursor glass shows the discharge capacity of 14 mAh g^{-1} at the rate of 1 μA cm^{-2} and the glass-ceramics with $Li_3V_2(PO_4)_3$ prepared with glucose at 700 °C in 7%H_2/Ar show the capacities of 117–126 mAh g^{-1} (~96% of the theoretical capacity) which are independent of heat treatment time. The present study proposes that the glass-ceramic processing is a fast synthesizing route for $Li_3V_2(PO_4)_3$ crystals.

© 2011 Elsevier B.V. All rights reserved.

1. Introduction

Lithium ion secondary batteries have been widely used as energy sources of laptop-type personal computers, mobile phones, and so on, because of advantages such as portability and high energy densities. At present, for instance, $LiCoO_2$ has been usually used as cathode materials in commercially available lithium ion secondary batteries. But its poor safety and high cost prohibit its use in large-scale devices such as electronic vehicles. From the view point of natural resources of transition metal oxides and of safety use of batteries, therefore other cathode materials not including cobalt element have received much attention.

Recently, lithium transition metal phosphates such as $LiFePO_4$ [1–4], $LiMnPO_4$ [5,6], $Li_3V_2(PO_4)_3$ [7–16], and $LiVOPO_4$ [17–19] have been proposed as potential cathode materials for lithium ion batteries. Monoclinic $Li_3V_2(PO_4)_3$ crystals exhibit excellent electrochemical performances such as the highest theoretical capacity (197 mAh g^{-1}) in phosphate cathodes reported and high-potentials of 3.60, 3.65, 4.10 V (for V^{4+}/V^{3+}) and 4.55 V (for V^{5+}/V^{4+}). In addition, the diffusion coefficient (D_{Li+}) of Li^+ ions in $Li_3V_2(PO_4)_3$ crystals is the order of $D_{Li+} = 10^{-9}$–10^{-10} cm^2 s^{-1} [20], which is much higher than that ($D_{Li+} = 10^{-14}$–10^{-15} cm^2 s^{-1}) in $LiFePO_4$ crystals [21]. These features ensure that $Li_3V_2(PO_4)_3$ can replace $LiCoO_2$ as practical battery cathode. On the other hand, phosphate materials have poor electronic conductivities, which limit charge–discharge rates for lithium ion batteries. This problem has been solved by controlling the morphology of cathode particles such as carbon coating [4,7,12–16,19,22], particle size reduction, controlling interface [23] and so on. To synthesize lithium vanadium phosphates with controlled morphology, various preparation methods have been proposed, which usually, however, require long preparation time, high cost reagents, and complicated preparation processes.

Very recently, the glass-ceramic processing route has been applied to synthesize phosphate-based lithium conductive materials such as $LiFePO_4$ [4,24–27], $LiVOPO_4$ [17,22], and $Li_3Fe_2(PO_4)_3$ [28]. The glass-ceramic technique has some advantages such as simple fabrication process, high-speed synthesis, no requirement of high cost reagent and so on. These advantages are preferable to practical applications in lithium ion secondary batteries. In previous study [17], the fabrication and crystallization behavior of Li_2O–V_2O_5–P_2O_5 glasses were examined to synthesize $LiVOPO_4$ crystals. During the crystallization of Li_2O–V_2O_5–P_2O_5 glasses, $LiVOPO_4$ and Li_2VPO_6 crystals were formed whereas $Li_3V_2(PO_4)_3$ was not formed, suggesting that V^{3+} ions does not exist in the glasses and in the glass-ceramics. That is, a reduction of vanadium ion by reducing agent is necessary to obtain V^{3+}-containing compounds in the glass-ceramic processing.

In this paper, we focus our attention on a synthesis of carbon-coated $Li_3V_2(PO_4)_3$ crystals by using a glass-ceramic processing. We prepared a glass with the composition of $37.5Li_2O$–$25V_2O_5$–$37.5P_2O_5$ corresponding to the stoichiometric

* Corresponding author. Tel.: +81 258 47 9313; fax: +81 258 47 9300.
E-mail address: komatsu@mst.nagaokaut.ac.jp (T. Komatsu).

0378-7753/$ – see front matter © 2011 Elsevier B.V. All rights reserved.
doi:10.1016/j.jpowsour.2011.06.094

composition of $Li_3V_2(PO_4)_3$ crystalline phase by a conventional melt-quenching method. The glass-ceramic powders coated with carbon was successfully obtained by means of a calcination of glucose in an electric furnace. We have optimized the synthesis condition concerning reduction heat treatments in the glass-ceramic processing and found that $Li_3V_2(PO_4)_3$ prepared with glucose at 700 °C in 7%H_2/Ar atmosphere shows the capacity of 117–126 mAh g^{-1} (~96% of the theoretical capacity).

2. Experimental

A glass with the composition of $37.5Li_2O$–$25V_2O_5$–$37.5P_2O_5$ (designated here as LVP323) corresponding to the composition of $Li_3V_2(PO_4)_3$ crystal was prepared by a conventional melt quenching method. Commercial powders of reagent grade $LiPO_3$ and V_2O_5 were mixed together as a molar ratio of 3:1. Then, the mixtures were melted at 1000 °C for 30 min in air using a platinum crucible in an electric furnace. The melts were poured onto an iron plate and pressed by another iron plate. The glass transition, T_g, and crystallization peak, T_p, temperatures were determined using differential thermal analyses (DTA: Rigaku Thermo plus TG8120) at a heating rate of 10 K min^{-1}. The plate glasses were pulverized by using a planetary ball-milling method (Fritsch premium line P-7), where zirconia pot and 5 mmϕ zirconia balls are used. X-ray photoelectron spectroscopy (XPS) measurements for vanadium ions were carried out with a SHIMADZU ESCA-3200 electron spectrometer which has the Al conical anode for charge controls. Non-monochromatic 240 W Mg Kα X-rays provided the excitation radiation. XPS spectra of the V2p core level of the glass surface were recorded. The drift of the electron binding energy (E_B) due to the surface charging effect was calibrated by utilizing the C1s peak of the contamination of the pumping oil (E_B = 284.6 eV).

The glass powders and glucose as a reducing agent were mixed and dispersed with ethanol. The suspension was dried in a dry oven at 80 °C. The mixtures were heat-treated at various temperatures (500–800 °C) under N_2 and 7%H_2/Ar atmospheres. The crystalline phases present in the crystallized samples were identified by X-ray diffraction (XRD) analyses (Cu Kα radiation) at room temperature. The XRD patterns were refined by Rietveld method by using RIETAN-FP software [29]. The morphology and the particle size for the precursor glass and the glass-ceramic powders were observed by using a scanning electron microscope (SEM; JIB-4500). Amounts of residual carbon formed in crystallization process were determined by the thermogravimetry (TG) measurements.

Electrical conductivities of the glass were evaluated using impedance spectroscopy measurements, in which silver paste was painted onto the surface of the samples as electrodes. The real (Z') part and imaginary (Z'') part for the samples were measured by an alternating current (AC) impedance method using an impedance analyzer (YHP 4192A) with the oscillation level of ±1 V in the frequency range of 5 Hz–13 MHz. The activation energy of the electrical conductivity was measured in the temperature range of 25–240 °C.

The electrochemical tests were performed in testing cell. Cathode composites were prepared by mixing 80 wt% glass–ceramics (for active material), 15 wt% acetylene black (for electronic conductor), and 5 wt% polyvinylidene difluoride (PVDF). The mixture was then pressed into an Al thin sheet, and circular disks were prepared by cutting the sheet. Stainless test cells were constructed using a lithium metal as an anode and an electrolyte of 1 M $LiPF_6$ consisting of a 1:1 solution of ethylene carbonate (EC) and diethyl carbonate (DEC). The lithium ion battery performance at room temperature was evaluated from charge/discharge measurements (Hokuto denko Co., HJ-1001). The cell potential was swept in the voltage range of 3–4.3 V, and the charge/discharge rate was 0.01–5 C.

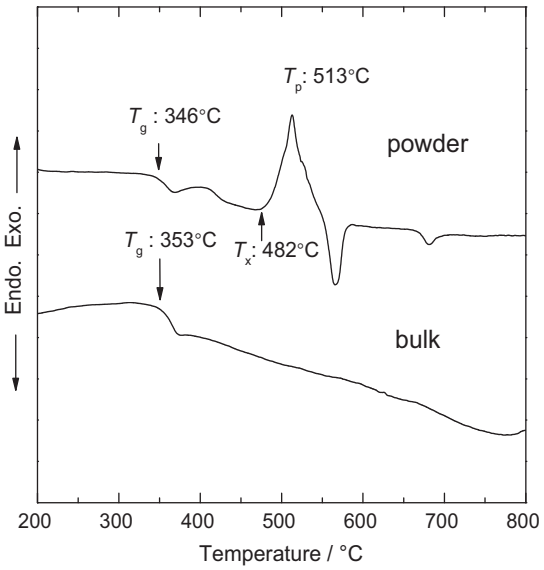

Fig. 1. DTA patterns for bulk and powdered LVP323 glass in air. A heating rate was 10 K min^{-1}.

3. Results and discussion

3.1. Feature of the precursor glass

In the XRD measurement for the melt-quenched sample, only a halo pattern without any sharp peak was observed, indicating that the melt-quenched sample with the composition of $37.5Li_2O$–$25V_2O_5$–$37.5P_2O_5$ is fully amorphous. Bulk and powder DTA patterns for the melt-quenched sample in air are shown in Fig. 1. In the DTA pattern for the bulk sample, an endothermic peak due to the glass transition was clearly observed, giving the value of the glass transition temperature, T_g = 353 °C. However, no crystallization peak was found in the temperature range of T_g–800 °C, suggesting that the melt-quenched bulk sample, i.e., LVP323 bulk glass, has a high thermal stability against crystallization. On the other hand, in the DTA pattern for the glass powder, an endothermic peak due to the glass transition and a broad exothermic peak due to the crystallization were found, giving the values of T_g = 353 °C and T_p = 513 °C. The DTA patterns shown in Fig. 1, therefore, indicate that the main crystallization mechanism in LVP323 glass is not bulk crystallization (homogeneous nucleation), but surface crystallization (inhomogeneous nucleation). The broad crystallization peak observed in the powder sample seems to be a superposition of several crystallization peaks, suggesting that several different crystalline phases will appear during heat treatment in air.

The XPS spectrum near the V2p levels for LVP323 glass is shown in Fig. 2. It is known that different valence states give different V2p-binding energies, i.e., around 516 eV for V^{4+} and around 517 eV for V^{5+}. The XPS spectrum for the precursor glass was decomposed into two components in order to know the fraction of vanadium ions as described in the former reports [17,30], in which the Voigt function was used. The result with a good fitting quality is also shown in Fig. 2, giving the values of 515.9 and 517.1 eV, which are assigned to V^{4+} and V^{5+} ions. The fraction of V^{4+} or V^{5+} was estimated from the ratio of the decomposed areas, and the fractions of vanadium ions were obtained to be V^{4+} = 11% and V^{5+} = 89%. In the previous study for $33.3Li_2O$–$33.3V_2O_5$–$33.3P_2O_5$ (LVP111) glass prepared by a melting at 1300 °C for 30 min, the fractions of V^{4+} and of V^{5+} were 48% and 52% [17]. Bacewicz et al. [31] reported that the fraction of V^{5+} increases with increasing V_2O_5 content in xLi_2O–$(100-2x)V_2O_5$–P_2O_5 glasses. In this study, however, the fraction of V^{5+} in LVP323 glass with the V_2O_5 content of

25 mol% is higher than that in LVP111 glass with the V_2O_5 content of 33.3 mol%. It should be pointed out that LVP323 glass was prepared in a melting condition of 1000 °C and 30 min. Generally, low melting temperature gives high valence state compared with high melting temperature for transition metal ions in a given glass. Even in Li_2O–V_2O_5–P_2O_5 glasses, therefore, it is considered that melting temperature affects strongly the valence of vanadium ions.

The electrical impedance measurements for the bulk LVP323 glass were carried out, and it was found that the electric conductivity (σ) of LVP323 glass at 20 °C is approximately $\sigma = 7.7 \times 10^{-9}$ S cm^{-1} and the activation energy (E_a) in the temperature range of 25–240 °C for LVP323 glass is $E_a = 0.54$ eV. The electrical conductivity of the $33.3Li_2O$–$33.3V_2O_5$–$33.3P_2O_5$ (LVP111) glass was reported to be $\sigma = 5 \times 10^{-10}$ S cm^{-1} at room temperature [17]. Jozwiak and Garbarczyk [32] reported that $35Li_2O$–$30V_2O_5$–$35P_2O_5$ glass shows the value of $\sigma \sim 10^{-8}$ S cm^{-1} at 50 °C. They also reported that Li_2O–V_2O_5–P_2O_5 glasses exhibit electronic (hopping in V^{4+}–O–V^{5+}), ionic (Li^+) or mixed electronic-ionic conductivities depending on composition. Very recently, Okada et al. [33] reported that the electrical conductivity of xLi_2O–$(70-x)Nb_2O_5$–$30P_2O_5$ glasses increases monotonously with increasing Li_2O content, e.g., $\sigma = 2.35 \times 10^{-6}$ S cm^{-1} for $60Li_2O$–$10Nb_2O_5$–$30P_2O_5$ glass, and the activation energy for Li^+ ion mobility in the temperature range of 25–200 °C is $E_a = 0.48$–0.58 eV. Considering the valence ($V^{5+} = 89\%$) of vanadium ion in LVP323 glass and the activation energy of $E_a = 0.54$ eV, the main carrier of the electrical conductivity in this LVP323 glass would be Li^+ ions.

3.2. Crystallization of LVP323 glass with glucose under N_2 gas flow

The mixtures of LVP323 glass powders and glucose (amount: 10 wt%) were crystallized by heat treatments at 500–800 °C for 6 h under N_2 gas flow, and the XRD patterns for the glass-ceramic powders obtained are shown in Fig. 3. All diffraction peaks are assigned to the $Li_3V_2(PO_4)_3$ crystalline phase with a monoclinic structure (space group: $P2_1/n$, JCPDS: 01-072-7074). The intensity of the peaks increases with increasing heat treatment temperature, indicating that the amount of $Li_3V_2(PO_4)_3$ crystals formed increases. It is noted that the formation of only $Li_3V_2(PO_4)_3$ crystals is confirmed even in the sample heat-treated at 500 °C, although the amount of $Li_3V_2(PO_4)_3$ crystals are small.

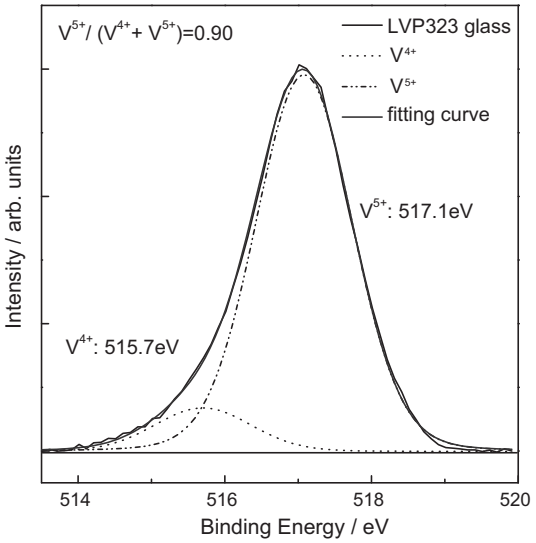

Fig. 2. XPS spectrum near the V2p levels at room temperature for LVP323 glass.

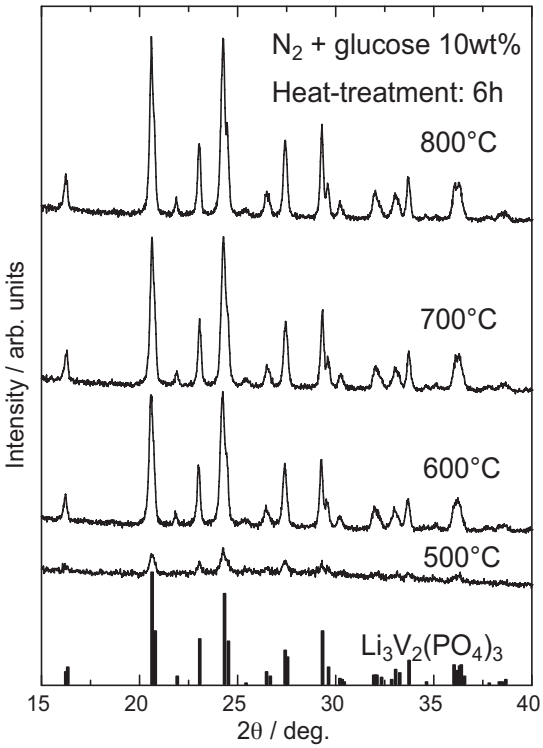

Fig. 3. XRD patterns for the glass-ceramic powders obtained by heat treatments with glucose (10 wt%) at 500–800 °C for 6 h in N_2 atmosphere.

It should be pointed out that the formation of other crystalline phases such as β-$LiVOPO_4$ with V^{4+} and Li_2VPO_6 with V^{5+} is not confirmed, as shown in Fig. 3. The results shown in Fig. 3, therefore, suggest that vanadium ions of V^{4+} and V^{5+} in the precursor LVP323 glass are reduced largely to V^{3+} ions during heat treatments with glucose under N_2 gas flow atmosphere. In other words, the added glucose is effectively working as reducing agent in the synthesis of $Li_3V_2(PO_4)_3$ crystals in the glass-ceramic processing. It has been reported that glucose added in Li_2O–Fe_2O_3–P_2O_5 glasses transforms into amorphous carbon during heat treatment in inert gas or reducing atmosphere and is effectively working in the reduction of Fe^{3+} to Fe^{2+} [4].

3.3. Crystallization of LVP323 glass with glucose under 7%H_2/Ar atmosphere

The LVP323 glass powders with glucose were heat treated at 500–700 °C for 6 h in 7%H_2/Ar atmosphere in order to examine the effect of reducing atmosphere on the formation of $Li_3V_2(PO_4)_3$ crystals. The XRD patterns for the crystallized samples obtained by heat treatments at 500–700 °C in 7%H_2/Ar atmosphere are shown in Fig. 4. All diffraction peaks are assigned to the $Li_3V_2(PO_4)_3$ crystalline phase. In particular, it is found that the sample heat-treated at 500 °C shows clearly the formation of $Li_3V_2(PO_4)_3$ crystals. Compared with the XRD patterns shown in Fig. 3 (in N_2 flow condition), it is, therefore, concluded that the combination of glucose addition and heat treatment under 7%H_2/Ar atmosphere is more effective for the synthesis of $Li_3V_2(PO_4)_3$ crystals, i.e., more effective for the reduction of V^{4+} or V^{5+} to V^{3+}.

The LVP323 glass powders with (10 wt%) and without glucose were heat-treated at 700 °C for 0.5–12 h in 7%H_2/Ar atmosphere, and the results are shown in Figs. 5 and 6. In the glass-ceramics obtained by heat treatments with glucose, only the $Li_3V_2(PO_4)_3$ crystalline phase was formed. It is noted that $Li_3V_2(PO_4)_3$ crystals are formed clearly even in the short heat treatment time of 0.5 h.

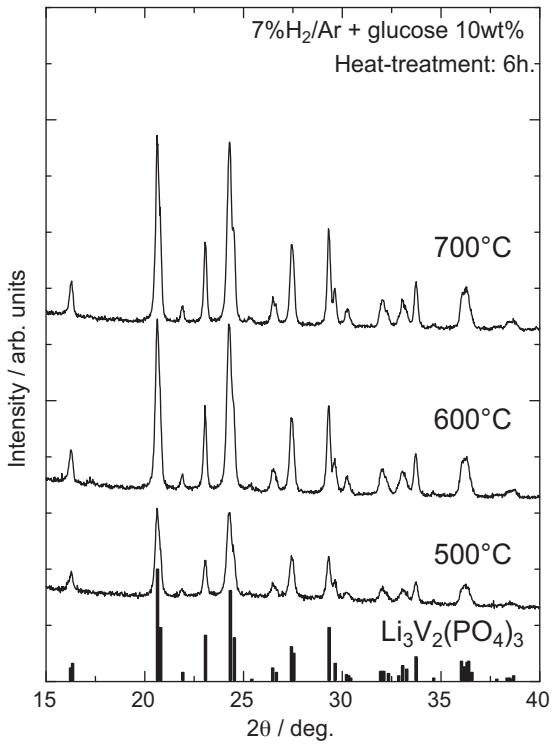

Fig. 4. XRD patterns for the glass-ceramic powders obtained by heat treatments with glucose (10 wt%) at 500–700 °C for 6 h in 7%H_2/Ar atmosphere.

On the other hand, in the condition of without glucose, the formation of $LiVP_2O_7$ crystals with V^{3+} is induced in the heat treatments of 0.5 and 3 h. In the heat-treated sample of 12 h, the formation of $LiVP_2O_7$ crystals is not confirmed anymore, suggesting that the $LiVP_2O_7$ phase might react with the glassy phase and transform into $Li_3V_2(PO_4)_3$ during the long time heat treatment of 12 h. It has been reported that vanadium ions in $LiVP_2O_7$ dissolve into the electrolyte on the charge–discharge cycle and thus cause capacity fading [34]. Thus the presence of $LiVP_2O_7$ crystals should be avoided in an application to lithium ion secondary batteries. These results indicate that the combination of glucose addition and 7%H_2/Ar atmosphere in the heat treatment process is effective not only for the reduction of V^{4+} or V^{5+} to V^{3+}, but also for the formation of $Li_3V_2(PO_4)_3$.

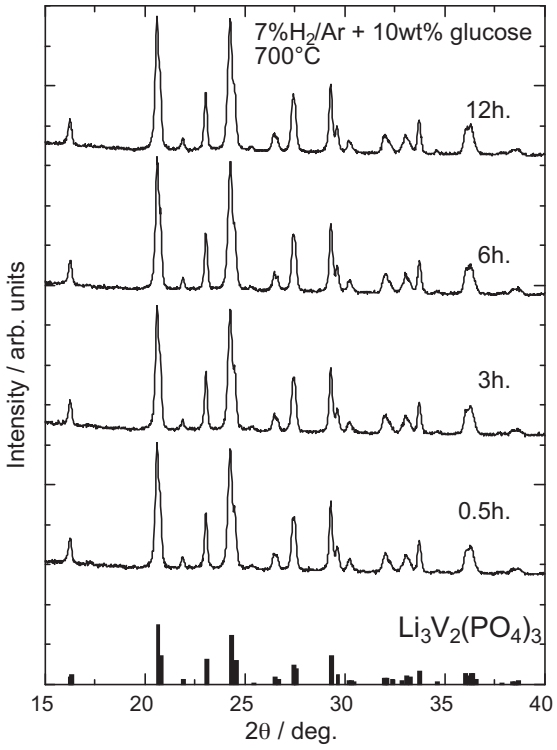

Fig. 5. XRD patterns for the glass-ceramic powders obtained by heat treatments with glucose (10 wt%) at 700 °C for 0.5–12 h in 7%H_2/Ar atmosphere.

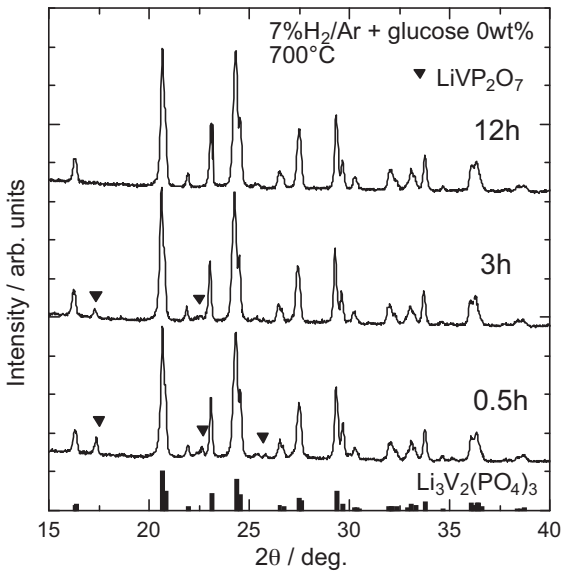

Fig. 6. XRD patterns for the glass-ceramic powders obtained by heat treatments at 700 °C for 0.5–12 h in 7%H_2/Ar atmosphere.

In the fabrication of Li^+ ion conductive materials, the lowering of fabrication temperature is one of the most important points. Fu et al. [11] reported that heat treatments (e.g., at 900 °C for 12 h) at high temperatures above 850 °C are needed for the synthesis of $Li_3V_2(PO_4)_3$ crystals in a solid-state reaction technique, because Li_3PO_4 crystals are formed at temperatures below 850 °C. It should be emphasized that glass-ceramic processing applied in this study requires the heat treatment at 700 °C for 0.5 h for the fabrication of $Li_3V_2(PO_4)_3$ crystals. The XRD pattern for the glass-ceramics obtained by the heat treatment at 700 °C for 0.5 h with glucose was refined by Rietveld method and the result is shown in Fig. 7. The lattice parameters for $Li_3V_2(PO_4)_3$ crystals in the glass-ceramics were calculated to be $a = 1.2050$ nm, $b = 0.8608$ nm, $c = 0.8612$ nm, $\beta = 90.518°$, and $V = 0.89331$ nm^3. These values are close to those ($a = 1.2037$ nm, $b = 0.8592$ nm, $c = 0.8606$ nm, $\beta = 90.61°$) reported by Yin et al. [35].

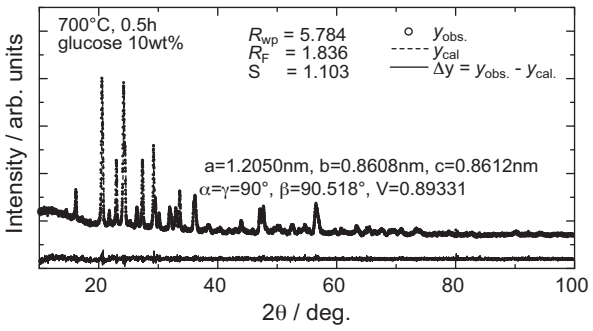

Fig. 7. X-ray Rietveld analysis results for the glass ceramics obtained by the heat treatment with glucose (10 wt%) at 700 °C for 0.5 h in 7%H_2/Ar atmosphere.

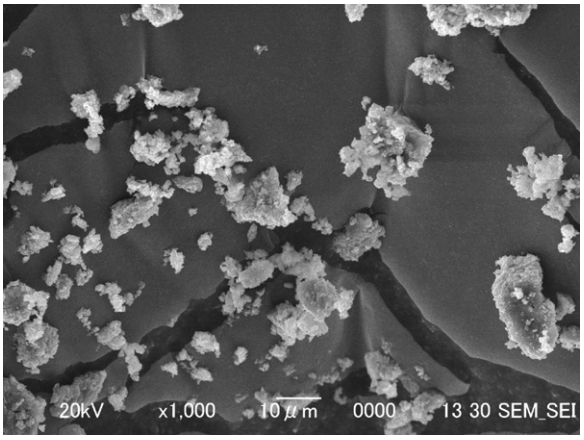

Fig. 8. SEM image for the precursor LVP323 glass powders prepared by a planetary ball milling.

The SEM image for the precursor glass powders obtained by using a planetary ball-milling method is shown in Fig. 8. It is seen that the primary particles with a diameter of 2–3 μm are present and they are gathered, giving the secondary particles with a diameter of 10–20 μm. The SEM image for the glass-ceramics obtained by the heat treatment with glucose (10 wt%) at 700 °C for 0.5 h is shown in Fig. 9. Besides small particles with a diameter of ~5 μm, large particles with a diameter of >20 μm were found. Such large particles might be formed due to the sintering and crystallization of small precursor glass powders and also due to the coating or taking of carbon in crystallized particles consisting of $Li_3V_2(PO_4)_3$ crystals.

3.4. Carbon content in the LVP323 glass-ceramics

The amount of carbon remained in the LVP323 glass-ceramics obtained by heat treatments at 700 °C for 0.5–12 h in 7%H_2/Ar atmosphere was estimated from TG–DTA measurements. The initial amount of glucose added to the precursor LVP323 glass was 10 wt%. The decrease in the weight (i.e., carbon content) was started at 350 °C, and the broad exothermic peak corresponding to the burning of glucose (carbon) was observed in the DTA curves. The values of carbon contents estimated by TG–DTA measurements are shown in Fig. 10 as a function of heat treatment time. These results do not include the effect of oxidation in vanadium ions because the oxidation of V^{3+} in $Li_3V_2(PO_4)_3$ will take place at above 527 °C (800 K)

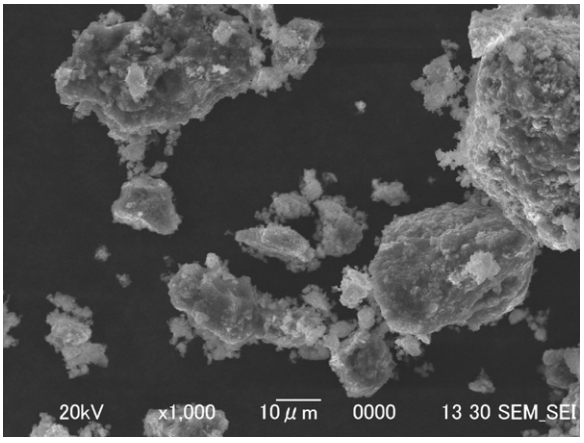

Fig. 9. SEM image for the glass-ceramic powders obtained by heat treatment with glucose (10 wt%) at 700 °C for 0.5 h in 7%H_2/Ar atmosphere.

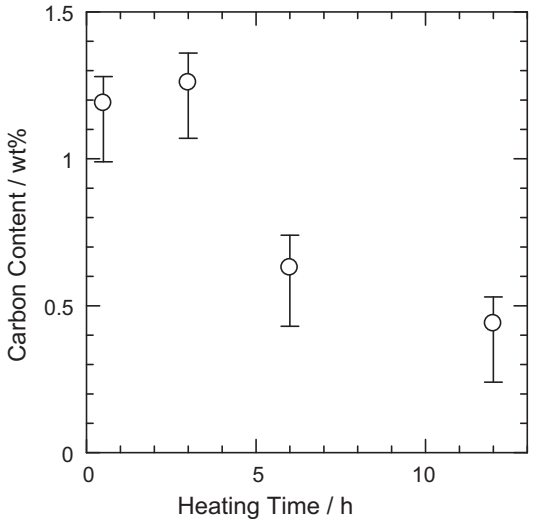

Fig. 10. Residual carbon contents estimated by using TG measurements for the LVP323 glass ceramics obtained by heat treatments at 700 °C for 0.5–12 h in 7%H_2/Ar atmosphere.

in air [36]. The carbon amounts for LVP323 glass ceramics at various treatment times were 0.3–1.3 wt%. The carbon content tends to decrease with increasing heat treatment time, and it might be suggested that carbon is consumed by some reactions during heat treatment.

3.5. Battery performances for the LVP glass and the glass-ceramics with $Li_3V_2(PO_4)_3$

The charge–discharge measurements for LVP323 glass powders at the voltage window of 1.0–4.3 V were carried out, and the results are shown in Fig. 11. The discharge capacity of LVP323 glass powders at the rate of 1 μA cm^{-2} was ~14 mAh g^{-1}. In discharge measurements, two plateaus at ~4 V and ~2 V were observed. In this glass, vanadium ions act as a redox center. It has been reported that α-$Li_xV_2O_5$ (x = 0–1) crystal shows two distinct voltage plateaus at 3.2 V and 3.4 V. On the other hand, Nabavi et al. [37] reported that the open circuit voltage continuously decreases with the amount of inserted Li^+, suggesting that no phase transition occurs in amorphous $Li_xV_2O_5$ up to x = 1.8. Although LVP323 glass powders used in the charge–discharge measurements were amorphous, two plateaus were observed in the discharge process. However, in the first charging process, no plateau was found. It might be suggested that some structure change occurs during the first charging pro-

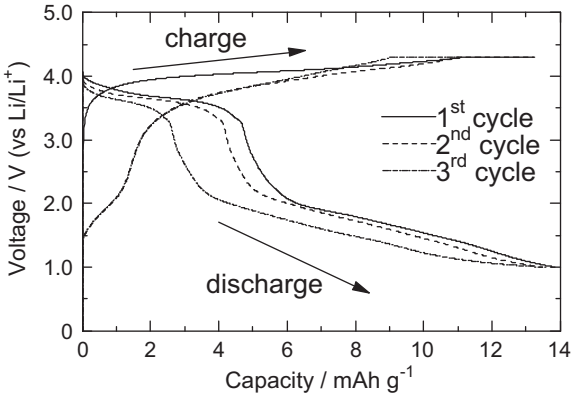

Fig. 11. Charge–discharge curves for LVP323 glass powders at the rate of 1 μA cm^{-2} in the range of 1.0–4.3 V.

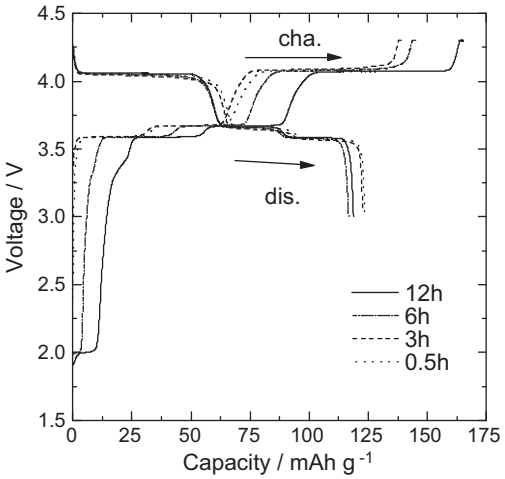

Fig. 12. Charge–discharge curves at the first cycle for LVP323 glass ceramic powders obtained by heat treatments with glucose (10 wt%) at 700 °C for 0.5–12 h at the rate of 0.01 C (1.97 mA g^{-1}) in the range of 3.0–4.3 V.

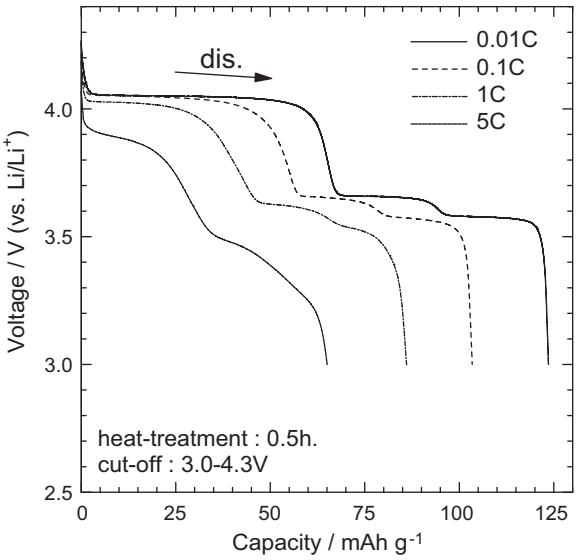

Fig. 13. Charge–discharge curves for LVP323 glass ceramic powders obtained by heat treatments with glucose (10 wt%) at 700 °C for 0.5 h at the rate of 0.01–5 C in the range of 3.0–4.3 V.

cess. Anyway, the discharge capacity for the LVP323 glass was very low even in the very slow rate (~8 μA). It would be due to the low electric conductivity of $\sigma = 7.7 \times 10^{-9}$ S cm^{-1}.

$Li_3V_2(PO_4)_3$ crystal has three extractable Li^+ ions placed on different crystallographic sites. It is, therefore, shown that four plateaus corresponding to the $x = 3$–2.5, 2.5–2, 2–1, and 1–0 of $Li_xV_2(PO_4)_3$ have the voltage of 3.6, 3.65, 4.1, and 4.55 V, respectively. In the high voltage charge process, an oxidation of electrolyte and a decrease of the cycle stability of cathode materials are inevitable. It causes loss in capacity. So, in order to focus only on a battery performance of the glass ceramics as a cathode, a voltage window was restricted to the range of 3.0–4.3 V in this measurements, where the theoretical capacity of $Li_xV_2(PO_4)_3$ ($x = 3$–1) is 132 mAh g^{-1}.

The charge–discharge curves at the rate of 0.01 C for the LVP323 glass-ceramics obtained by heat treatments with glucose at 700 °C for various times (0.5–12 h) in 7%H_2/Ar atmosphere are shown in Fig. 12. Three plateaus were clearly observed at around 3.6, 3.65, and 4.1 V corresponding to $2Li^+$. The discharge capacities for the LVP323 glass ceramics obtained were 117–126 mAh g^{-1} and were independent of heat treatment time. These results show that $Li_3V_2(PO_4)_3$ crystals are sufficiently formed even in the heat treatment of the short time of 0.5 h and the glass-ceramics obtained is working as cathode active materials. The samples obtained by heat treatments of 3–12 h have small plateaus at around 2 V in charge curves. The regions of plateaus at 2 V increased with increasing heat treatment time. It have been reported that V^{3+} in $Li_3V_2(PO_4)_3$ is reduced into V^{2+} with Li^+ insertion and the redox effect occurs at around 2 V [36]. Therefore, the small plateau at 2 V observed in those samples might be due to the existence of V^{2+} ions in the glass-ceramics. These results also indicate that the glass-ceramic processing is a fast, simple and useful method to fabricate $Li_3V_2(PO_4)_3$ crystals. The discharge curves at the various charge–discharge rates (0.01–5 C) for the LVP323 glass-ceramics obtained by the heat treatment of 0.5 h are shown in Fig. 13. The discharge capacities at 0.01, 0.1, 1, and 5 C were found to be 125, 103, 89, and 71 mAh g^{-1}, respectively. It is seen that the discharge capacity for the glass-ceramics decreases with increasing charge–discharge rate. When the charge and discharge were operated at above 1 C, the effect of overvoltage became larger and the plateaus became unclear, indicating that the electric conductivity of the glass-ceramics is insufficient for high rate charge–discharge conditions.

4. Conclusions

The synthesis of $Li_3V_2(PO_4)_3$ crystals for lithium ion secondary batteries via the glass-ceramic processing was carried out. It was revealed from XPS measurements that the valence of vanadium ions in the precursor LVP323 glass is mainly V^{5+}, i.e., 90%. It was found that heat treatments with glucose (10 wt%) in 7%H_2/Ar atmosphere give effectively the formation of $Li_3V_2(PO_4)_3$ crystals. The discharge capacities for the LVP323 glass ceramics obtained by heat treatments at 700 °C in 7%H_2/Ar atmosphere were 117–126 mAh g^{-1}, indicating that the glass-ceramics with $Li_3V_2(PO_4)_3$ is working as cathode active materials. The present study demonstrates that the glass-ceramic processing is a fast, simple and useful method for the fabrication of $Li_3V_2(PO_4)_3$ crystals.

Acknowledgements

This work was supported by Grants-in-Aid for Scientific Research from the Ministry of Education, Science, Sports, Culture, and Technology, Japan, and the Program for Developing the Supporting System for Global Multidisciplinary Engineering Establishment in Nagaoka University of Technology. One (K. Nagamine) of the authors thanks JSPS Research Fellowships for Young Scientists.

References

[1] A.K. Padhi, K.S. Nanjundaswamy, J.B. Goodenough, J. Electrochem. Soc. 14 (1997) 1188–1194.
[2] A. Yamada, S.C. Chung, J. Electrochem. Soc. 148 (2001) A960–A967.
[3] A. Yamada, S.C. Chung, K. Hinokuma, J. Electrochem. Soc. 148 (2001) A224–A229.
[4] T. Honma, K. Hirose, T. Komatsu, T. Sato, S. Marukane, J. Non-Cryst. Solids 356 (2010) 3032–3036.
[5] G. Li, H. Azuma, M. Tohda, Electrochem. Solid-State Lett. 5 (2002) A135–A137.
[6] A. Yamada, M. Hosoya, S.C. Chung, Y. Kudo, K. Hinokuma, K.Y. Liu, Y. Nishi, J. Power Sources 119–121 (2003) 232–238.
[7] H. Huang, S.C. Yin, T. Kerr, N. Taylor, L.F. Nazar, Adv. Mater. 14 (2002) 1525–1528.
[8] M. Sato, H. Ohkawa, K. Yoshida, M. Saito, K. Uematsu, K. Toda, Solid State Ionics 135 (2000) 137–142.
[9] Y.Q. Qiao, X.L. Wang, Y. Zhou, J.Y. Xiang, D. Zhang, S.J. Shi, J.P. Tu, Electrochim. Acta 56 (2010) 510–516.
[10] M.Y. Saidi, J. Barker, H. Huang, J.L. Swoyer, G. Adamson, Electrochem. Solid-State Lett. 5 (2002) A149–A151.
[11] P. Fu, Y. Zhao, Y. Dong, X. An, G. Shen, J. Power Sources 162 (2006) 651–657.
[12] X.H. Rui, C. Li, J. Liu, T. Cheng, C.H. Chen, Electrochim. Acta 55 (2010) 6761–6767.

[13] Y.N. Ko, H.Y. Koo, J.H. Kim, J.H. Yi, Y.C. Kang, J.-H. Lee, J. Power Sources 196 (2011) 6682–6687.
[14] Y.Q. Qiao, J.P. Tu, J.Y. Xiang, X.L. Wang, Y.J. Mai, D. Zhang, W.L. Liu, Electrochim. Acta 56 (2011) 4139–4145.
[15] X.H. Rui, N. Yesibolati, C.H. Chen, J. Power Sources 196 (2011) 2279–2282.
[16] Y.Q. Qiao, J.P. Tu, X.L. Wang, D. Zhang, J.Y. Xiang, Y.J. Mai, C.D. Gu, J. Power Sources 196 (2011) 7715–7720.
[17] K. Nagamine, T. Honma, T. Komatsu, J. Am. Ceram. Soc. 91 (2008) 3920–3925.
[18] K.H. Lii, C.H. Li, C.Y. Cheng, S.L. Wang, J. Solid State Chem. 95 (1991) 352–359.
[19] J. Barker, M.Y. Saidi, J.L. Swoyer, J. Electrochem. Soc. 151 (2004) A796–A800.
[20] X.H. Rui, N. Ding, J. Liu, C. Li, C.H. Chen, Electrochim. Acta 55 (2010) 2384–2390.
[21] P.P. Prosini, M. Lisi, D. Zane, M. Pasquali, Solid State Ionics 148 (2002) 45–51.
[22] K. Nagamine, T. Honma, T. Komatsu, IOP Conf. Ser.: Mater. Sci. Eng. 21 (2011).
[23] B. Kang, G. Ceder, Nature 458 (2009) 190–193.
[24] T. Honma, K. Nagamine, T. Komatsu, Ceram. Int. 36 (2010) 1137–1141.
[25] K. Hirose, T. Honma, Y. Benino, T. Komatsu, Solid State Ionics 178 (2007) 801–807.
[26] K. Hirose, T. Honma, Y. Doi, Y. Hinatsu, T. Komatsu, Solid State Commun. 146 (2008) 273–277.
[27] K. Nagamine, S. Reinsch, R. Mueller, T. Honma, T. Komatsu, J. Am. Ceram. Soc., in press.
[28] K. Nagamine, K. Hirose, T. Honma, T. Komatsu, Solid State Ionics 179 (2008) 508–515.
[29] F. Izumi, K. Momma, Solid State Phenom. 130 (2007) 15–20.
[30] N. Alov, D. Kutsko, I. Spirovov, Z. Bastl, Surf. Sci. 600 (2006) 1628–1631.
[31] R. Bacewicz, M. Wasiucionek, A. Twarog, J. Filipowicz, P.J. Jozwiak, J. Garbarczyk, J. Mater. Sci. 40 (2005) 4267–4270.
[32] P. Jozwiak, J.E. Garbarczyk, Solid State Ionics 176 (2005) 2163–2166.
[33] T. Okada, T. Honma, T. Komatsu, Mater. Res. Bull. 45 (2010) 1443–1448.
[34] C. Wurm, M. Morcrette, G. Rousse, L. Dupont, C. Masquelier, Chem. Mater. 14 (2002) 2701–2710.
[35] S.C. Yin, H. Grondey, P. Strobel, M. Anne, L.F. Nazar, J. Am. Chem. Soc. 125 (2003) 10402–10411.
[36] S. Patoux, C. Wurm, M. Morcrette, G. Rousse, C. Masquelier, J. Power Sources 119–121 (2003) 278–284.
[37] M. Nabavi, C. Sanchez, F. Taulelle, J. Livage, A. de Guibert, Solid State Ionics 28–30 (1988) 1183–1186.